Homogeneous superconducting phase in TiN film: A complex impedance study

P. Diener, H. Schellevis, and J. J. A. Baselmans

Citation: Appl. Phys. Lett. **101**, 252601 (2012);
View online: https://doi.org/10.1063/1.4771995
View Table of Contents: http://aip.scitation.org/toc/apl/101/25
Published by the American Institute of Physics

Homogeneous superconducting phase in TiN film: A complex impedance study

P. Diener,[1,a)] H. Schellevis,[2] and J. J. A. Baselmans[1]
[1]*SRON Netherlands Institute for Space Research, 3584 CA Utrecht, The Netherlands*
[2]*Delft Institute of Microsystems and Nanoelectronics, Delft University of Technology, 2628 CD Delft, Netherlands*

(Received 26 June 2012; accepted 28 November 2012; published online 17 December 2012)

The low frequency complex impedance of a high resistivity 92 $\mu\Omega$ cm and 100 nm thick TiN superconducting film has been measured via the transmission of several high sensitivity GHz microresonators, down to $T_C/50$. The temperature dependence of the kinetic inductance follows closely BCS local electrodynamics, with one well defined superconducting gap. This evidences the recovery of a homogeneous superconducting phase in TiN far from the disorder and composition driven transitions. Additionally, we observe a linearity between resonator quality factor and frequency temperature changes, which can be described by a two fluid model. © *2012 American Institute of Physics*. [http://dx.doi.org/10.1063/1.4771995]

Thin films of titanium nitride (TiN) have recently been proposed[1] for radiation detection using kinetic inductance detectors.[2] TiN and other strongly disordered superconducting materials have a high surface impedance for radiation with a photon energy $h\nu > 2\Delta$, which allows highly efficient radiation absorption. Additionally, disordered superconductors have a long magnetic penetration depth. This results in a relatively large value of the kinetic inductance, which increases the responsivity of the devices.

Recent work has revealed strong deviations from standard BCS theory for superconductors with a normal state resistivity in the range of 100 $\mu\Omega$ cm and higher,[3] clearly in violation of the Anderson theorem, which states that disorder does not affect the properties of the superconducting state.[4] These deviations increase with higher disorder, leading to systems in which a superconductor insulator transition (SIT) is observed, typically when the Ioffe-Regel parameter $k_F\ell \sim 1$. SITs have been observed in thin films of several materials by changing the disorder via a film treatment, or by varying the thickness, the film stoichiometry or the applied magnetic field.[5–8] In TiN, a SIT has been evidenced few years ago in ~5 nm thick films by magnetic field and thickness changes.[9,10] Several studies also report the presence of an inhomogeneous superconducting phase close to the SIT.[11–15]

One expects to recover a classical BCS superconducting phase when going to lower disorder/thicker films. In contrast, the only one spectroscopic study on a low disordered TiN film reports on the presence of a non uniform state comprising of superconducting and normal areas.[16] These results are discussed in the context of mesoscopic fluctuations close to a superconducting to normal transition. Indeed, TiN also exhibits a transition with composition: as reported recently, superconductivity disappears in the N sub stoichiometric range.[1] The presence of an inhomogeneous order parameter in a low disordered TiN film points out the necessity to disentangle the thickness and composition transitions.

In this paper, we report on the complex impedance study of several microresonators made of a 100 nm thick, relatively weakly disordered TiN film, having $k_F\ell = 12.7$ and a resistivity of 92 $\mu\Omega$ cm. The film has been characterized extensively, and the resonators have internal quality factors up to 10^7. This allows an accurate determination of the superconducting gap from the temperature resonance frequency shift, which is directly proportional to the kinetic inductance or superfluid density changes.

The film has been prepared by a DC magnetron sputtering system. It is sputtered on a nitrogen/argon plasma at 350 °C on a high resistive HF cleaned silicon substrate (see Ref. 17 for more details on the recipe). The thickness determined with a scanning electron microscope is $d = 100 \pm 5$ nm. The homogeneity has been checked by X-ray photoelectron spectroscopy (XPS) depth profiling: as shown in Fig. 1, there is no contamination except some oxygen at the surface on few nm, and the Ti/N ratio is thickness independent. The stoichiometry determined is 1:1.3 with an uncertainty of 20% related to the XPS calibration. There is a 1 GPa stress in the film, to obtain a dense and homogeneous

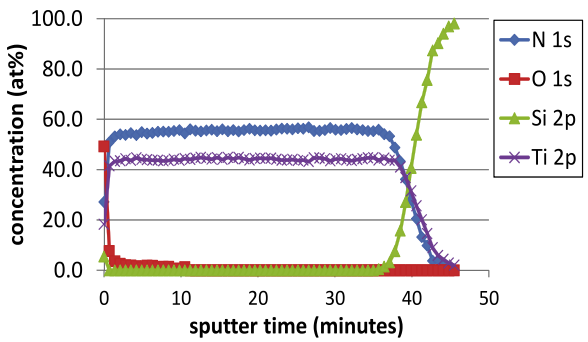

FIG. 1. Concentration-depth profiles measured by XPS depth profiling. The sputter rate calibrated in SiO_2 at the used setting of the ion gun was 4.4 nm/min. A small oxygen contamination is observed at the surface (left) on few nm, and the Ti and N concentrations remain constant in the film up to the Si substrate (right). The measured stoichiometry is 1:1.3 with, however, an important error due to the 20% uncertainty on the absolute concentration values with this technique.

a)diener@lps.u-psud.fr.

granular morphology.[17] This affects the unit cell size of 4.35 Å determined by X-ray diffraction (XRD), to be compared to the bulk value 4.24 Å. XRD spectra also show a favored (200) crystalline orientation. A typical grain size of 10 nm has been determined by transmission electron microscopy in others TiN films from the same source.[17]

The film characterizations at low temperature include standard R(T) and Hall measurements. The resistivity at 10 K, $\rho = 92\,\mu\Omega\,\text{cm}$ is almost constant up to 300 K and the carrier density is $n_0 = 3.77 \times 10^{22}\,\text{cm}^{-3}$. $k_F\ell$ can be estimated in the free electron model from ρ and n_0 by[18] $k_F\ell = 3\pi^2\hbar/(e^2\rho\sqrt[3]{3\pi^2 n_0})$ giving 12.7 for this film. In addition, Fig. 2 shows the sharp superconducting transition observed at $T_C = 4.38 \pm 0.01$ K.

Coplanar waveguide resonators (CPW) have been patterned using standard contact lithography and dry etching with an SF_6/Ar gas mixture. One resonator is shown Fig. 2. The resonators are formed by a central meandered line of few mm length, 3 μm wide, and slits of 2 μm wide between the central line and the groundplane. They are capacitively coupled to the feedline by placing one resonator end alongside it. The feedline is connected to coaxial cables at both chip sides and its S_{21} transmission is measured using a standard vector network analyzer. A detailed description of the setup can be found in Ref. 19.

Each resonator gives rise to a dip in S_{21} at a frequency $f_0^{-1} = 2\pi x l\sqrt{(L_k + L_g)C}$, with l the resonator length, L_k and L_g the kinetic and geometric inductance per unit length, and C the capacitance per unit length. x is a factor depending on the resonator type. Here, half of the resonators are halfwaves (open ended on both sides) corresponding to $x = 2$, the others are quarterwaves (short ended on one side) thus $x = 4$. The inductance per unit length is proportional to the surface inductance: $L_s = L_k/g$ with g a factor depending on the resonator geometry.[3] When the temperature is increased, Cooper pairs are broken by thermal excitations above the gap, resulting in a change of the kinetic inductance. This translate into a resonance frequency shift (see Fig. 2) and

$$\frac{\delta f(T)}{f} = -\frac{\alpha}{2}\frac{\delta L_k(T)}{L_k} = -\frac{\alpha}{2}\frac{\delta L_s(T)}{L_s}, \tag{1}$$

with $\alpha \equiv L_k/(L_k + L_g)$ the kinetic inductance ratio. For high $L_k \sim L_g$ films like the TiN film studied here, α is large enough to be determined precisely from the ratio of the experimental resonance frequency at the lowest temperature f_0 and the geometrical frequency f_g calculated from the CPW dimensions.[20]

To choose the correct model for $L_s(T)$, we first estimate several characteristic lengths. The London magnetic penetration depth $\lambda_L \approx 47$ nm is determined from the measured n_0 and using a quasiparticle mass m^* equal to 3 times the electron mass.[21] The BCS coherence length $\xi_0 = \frac{\hbar v_F}{\pi\Delta} \approx 120$ nm is estimated *a priori* using a gap $\Delta = 1.76\,k_B T_C$ and a Fermi velocity $v_F = \frac{\hbar\sqrt[3]{3\pi^2 n_0}}{m^*}$. The mean free path $\ell = \tau v_F = \frac{m^*}{n_0 e^2 \varrho}$ $v_F \approx 1$ nm is calculated from the measured ϱ_0 and n_0. We are now in position to estimate the effective coherence length $\xi_{eff} = (\xi_0^{-1} + \ell^{-1})^{-1} \approx 1.0$ nm and the magnetic penetration depth $\lambda_{eff} = \lambda_L(1 + \frac{\xi_0}{\ell})^{1/2} \approx 517$ nm. The film studied here is in the local ($\xi_{eff} \ll \lambda_{eff}$), dirty ($\ell \ll \xi_0, \lambda_L$), three dimensional ($\xi_{eff} \ll d$) and thin film limit ($d \ll \lambda_{eff}$). In thin films, the current is distributed uniformly and the relation between the square inductance and λ_{eff} simply reduces to

$$L_s = \mu_0 \frac{\lambda_{eff}^2}{d}. \tag{2}$$

In the local dirty limit and at $T < T_c/3$, the temperature dependence of λ_{eff} is given by[22]

$$\frac{\lambda_{eff}(T)}{\lambda_{eff}(0)} = \tanh\left(\frac{\Delta_0}{2k_B T}\right)^{-1/2}, \tag{3}$$

with Δ_0 the superconducting gap at zero temperature. This is valid in the low frequency limit $hf \ll 2\Delta_0$. It is verified here, since the frequency range used is 3–5.3 GHz corresponding to 12–22 μeV, which is less than 2% of the gap energy. Combining Eqs. (1)–(3), one obtains

$$\frac{\delta L_s}{L_{s0}} = -\frac{2}{\alpha}\frac{\delta f}{f_0} = 2\left(\tanh\left(\frac{\Delta_0}{2k_B T}\right)^{-1/2} - 1\right), \tag{4}$$

where f, L_s, and λ_{eff} have been replaced by their value at the lowest experimental temperature f_0, L_{s0}, and λ_{eff0} which is correct for $\delta L_{(s)} \ll L_{s0}$ and $\delta\lambda_{eff}(T) \ll \lambda_{eff0}$. This is valid for all temperatures below $T \sim 0.9\,T_c$, temperature above which the magnetic penetration depth diverges. As shown in Eq. (4), the temperature dependence of the resonance frequency shift is a direct probe of the superconducting gap.

The S_{21} transmission of 8 resonators of the same chip has been measured between 90 mK and 1 K. At low temperature, the internal quality factors are between 10^6 and 10^7. These high values support the conclusions of Ref. 23 on the relation between high quality factors and a (200) crystalline orientation in TiN films. The (f_0/f_g) ratio calculated from the

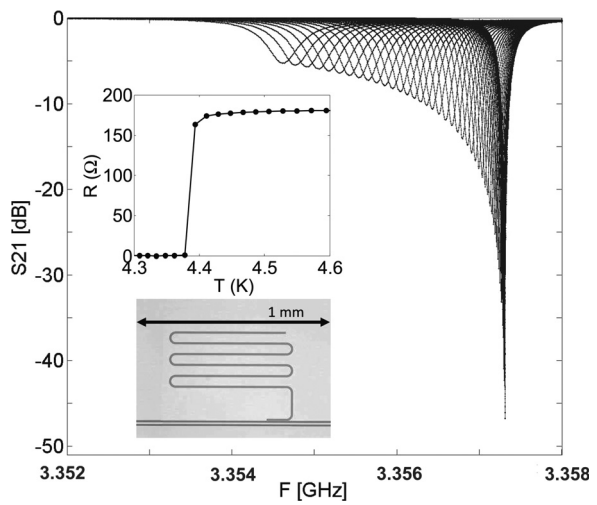

FIG. 2. Typical S_{21} transmission of one resonator for several temperatures between 90 mK and 1 K. When increasing T, the frequency and the quality factor decrease due to quasiparticle excitations above the gap. Upper inset: resistive superconducting transition. Lower inset: photo of one resonator from another chip having the same design. The meandered resonator line (light grey) is separated to the groundplane all around (light grey) by slits (dark grey) and is capacitively coupled to the feedline (lower straight line).

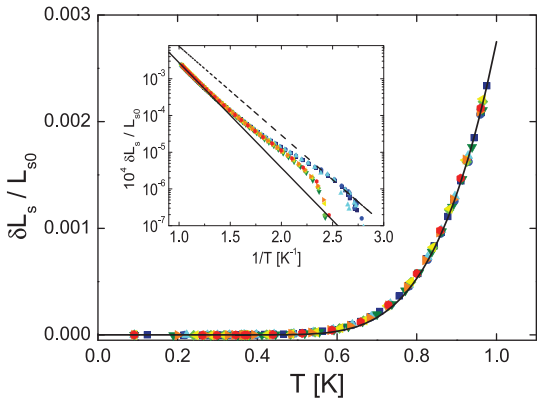

FIG. 3. Temperature dependence of the normalized surface inductance for the 8 resonators, having $f_0 = 3.28\,\text{GHz}$ (■), 3.36 GHz (●), 3.41 GHz (▲), 3.46 GHz (▼), 3.52 GHz (◆), 4.79 GHz (◀), 5.01 GHz (▶), 5.23 GHz (●). The black line is the best fit with Eq. (4) giving the gap value $\Delta = 0.57\,\text{meV}$. Inset: same curves in semi-log and inverse temperature scales to magnify the results at the lowest temperatures. The dotted line is Eq. (4) with $\Delta = 0.48\,\text{meV}$.

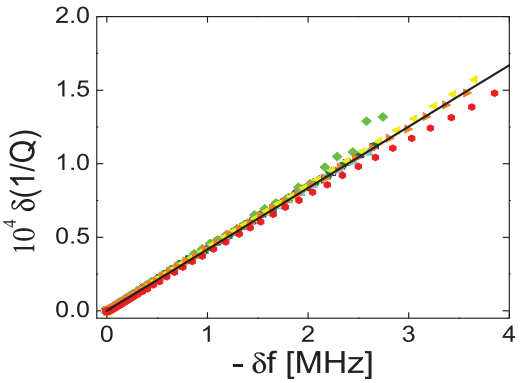

FIG. 4. Inverse of the quality factor $\delta(1/Q)(T)$ as a function of the frequency shift $\delta f(T)$ for the 8 resonators (same symbols as Fig. 3) between 90 mK and 1 K. The black line is a linear fit with Eq. (9) with $\tau = 1.7\,\text{ps}$.

measured f_0 is the same for all resonators, giving $\alpha = 1 - (f_0/f_g)^2 = 0.69$. $\delta L_s/L_{s0}(T)$ is shown in Fig. 3 for all resonators. They exhibit the same temperature dependence and an excellent fit is obtained with Eq. (4), giving $\Delta = 0.57\,\text{meV}$. There is, however, a slightly weaker curvature of the measured $\delta L_s/L_{s0}(T)$ below 0.6 K, which is magnified in log scale in the inset. The curves are between the values expected for $\Delta = 0.48\,\text{meV}$ and $\Delta = 0.57\,\text{meV}$, which may be attributed to a small gap decrease close to the film surfaces due to oxidization or stoichiometry changes, see Fig. 1. The inflexion point around $T \sim 0.45\,\text{K}$, followed below by a cut-off of the inductance shift which is not identical for all resonators/frequencies, is due to the capacitive dielectric variations[24] which becomes non negligible compared to the inductive changes in this temperature range. Comparing Δ and the critical temperature $T_C = 4.38\,\text{K}$, one obtains a ratio $\Delta/k_BT_C = 1.50$, lower than the BCS weak coupling ratio 1.76. This has nothing to do with the SIT: in contrast, as observed by Sacepe *et al.* in TiN ultra thin films,[12] one expects disorder to possibly increase Δ/k_BT_C close to the transition. The 1.50 ratio may be related to an effect of the grain size: as reported by Bose *et al.*[25] in niobium thick films, the critical temperature decreases when decreasing the grain size and the Δ/k_BT_C ratio is slightly reduced, going to 1.61 for 18 nm grains. A superconductivity weakening can also occur due to interface tunnel exchange at internal and external surfaces[26] as observed in niobium thin films.[27] This may also explain why all T_C reported for TiN films are below 4.8 K, whereas $T_C = 6.0\,\text{K}$ in a TiN single crystal.[28]

To go further, we have also compared the temperature dependence of the frequency and the quality factor Q. Fig. 4 shows the temperature dependence of the normalized quality factors $\delta(1/Q)(T) = (1/Q)(T) - (1/Q)(T=0)$ for all resonators as a function of the frequency shift—$df(T)$. The 8 resonators give similar results, and exhibit a linear behaviour. In the following, we show how this proportionality between quality factor and frequency shift can be reproduced analytically in the context of the two fluid model. In general, the radio frequency absorption cannot be described by local electrodynamics even at low temperature and low frequency, due to the non trivial form of the momentum transition matrix M.[29] This holds here, however, since we are only interested in the temperature dependence $\delta(1/Q)(T)$ and because M is temperature independent at $T < T_c/3$, where the gap and BCS coherence length remain unchanged.

Q is related to the surface impedance $Z_S = R_S + i\omega L_S$ by $Q = \omega L_{total}/R_{total} = \omega L_S/\alpha R_S$, with R_S the surface resistance. In the thin film limit, Z_S is simply related to the complex conductivity $\sigma = \sigma_1 + i\sigma_2$ by $Z_s^{-1} = \sigma d$. At low temperature, $\sigma_1 \ll \sigma_2$ and we get $R_S = \frac{\sigma_1}{\sigma_2^2 d}$ and $L_S = \frac{1}{\omega\sigma_2 d}$. The complex conductivity in the two fluid model is given by[22]

$$\sigma = \frac{n_n e^2 \tau}{m^*} \frac{1}{1 - i\omega\tau} + i\frac{n_s e^2}{m^* \omega}, \tag{5}$$

with n_n the quasiparticle density and τ the momentum relaxation time. In the limit $\omega\tau \ll 1$, one gets for the quality factor

$$\frac{1}{Q} = \alpha\frac{\sigma_1}{\sigma_2} = \alpha\omega\tau\frac{n_n}{n_S}. \tag{6}$$

The first part of Eq. (6) is identical to the equation used by Gao *et al.*[30] in the context of the Mattis Bardeen theory. Using the properties $n_n = \delta n_n$, $\delta n_n/\delta n_s = -2$, it becomes

$$\frac{1}{Q}(T) = -2\alpha\omega\tau\frac{\delta n_S(T)}{n_S}. \tag{7}$$

The quality factor temperature dependence is directly related to the superfluid density changes, as for the kinetic inductance: $L_S(T) = \frac{m}{2n_S(T)e^2 d}$ and

$$\frac{\delta n_S}{n_S} = -\frac{\delta L_s}{L_s} = \frac{2}{\alpha}\frac{\delta f}{f}. \tag{8}$$

By combining Eqs. (7) and (8), we obtain the relation between Q and δf

$$\frac{1}{Q} = -8\pi\tau\,\delta f. \tag{9}$$

As shown in Eq. (9), the inverse quality factor is proportional to the frequency shift and momentum relaxation time. This

means that losses, which are expected to be zero at zero temperature, increase proportionally to the quasiparticle density changes $\delta f \propto \delta n_n$, via the two fluid property $\delta n_n \propto \delta n_s$. In practice, there are always residual losses $1/Q(T=0)$ due to non equilibrium excess quasiparticles,[31,32] which are subtracted in Fig. 4. Fitting the results with Eq. (9) gives the momentum relaxation time at $T \ll T_c$, $\tau = 1.7\,10^{-12}\,s$. This is three orders of magnitude longer than in the metallic state $\tau_m = m^*/n_0 e^2 \rho = 3.0 \times 10^{-15}$ s estimated from the resistivity and the carrier density measured at 10 K. In the superconducting state, indeed, the momentum relaxation time strongly increases, typically up to $\sim 10^{-12}$ s in usual BCS superconductors[22] due to the quasiparticles vanishing by Cooper pair condensation.

The temperature dependence of the resonators' frequencies and quality factors clearly evidences the presence of one well defined superconducting gap in the density of states. Moreover, the excellent reproducibility between the resonators evidences the good superconducting phase homogeneity in the film. This differs from previous STM/S results on a similar 100 nm thick high $T_C = 4.68$ K TiN film, which report on the presence of an inhomogeneous superconducting phase having local normal areas. As discussed in Ref. 16, the detected inhomogeneous gap may be due to mesoscopic fluctuations at the proximity of a superconductor to metal transition. Indeed, the presence of a composition driven transition in TiN_x has been reported recently,[1] with a disappearance of the superconducting phase in the low x range, recovered at $x = 0$ (titanium). However, the film used in Ref. 16 has the characteristic high critical temperature of overstoichiometric TiN, similar to the one of the film measured here, and our results do not exhibit any signature of the proximity with the composition transition. Additionally, the granular morphology of the two films is different. Indeed, the film recipe used here has been especially developed to obtain densely packed grains in the film, corresponding to zone T in the Thornton classification. As discussed in Ref. 17, a typical low stress TiN film is of zone 1, containing many voids between grains. This may lead to important Josephson barriers between superconducting grains, which are expected to play a major role in the homogeneity of the superconducting phase of such systems even at relatively low disorder.[33]

In conclusion, the low frequency complex surface impedance has been studied on microresonators made from a thick overstoichiometric TiN film. The resonators' high quality factors allow a high sensitivity determination of the inductive and resistive changes with temperature. In contrast to the previous spectroscopic study in a similar film, all our results are in agreement with a homogeneous superconducting phase having a gap $\Delta = 0.57\,\text{meV} = 1.50 k_B T_C$.

We thank T. M. Klapwijk, A. Endo, E. F. C. Driessen, P. C. J. J. Coumou, R. R. Tromp, and S. J. C. Yates for support and fruitful discussions.

[1]H. G. Leduc, B. Bumble, P. K. Day, B. H. Eom, J. Gao, S. Golwala, B. A. Mazin, S. McHugh, A. Merrill, D. C. Moore *et al.*, Appl. Phys. Lett. **97**, 102509 (2010).
[2]P. K. Day, H. G. LeDuc, B. A. Mazin, A. Vayonakis, and J. Zmuidzinas, Nature **425**, 817 (2003).
[3]E. F. C. Driessen, P. C. J. J. Coumou, R. R. Tromp, P. J. de Visser, and T. M. Klapwijk, Phys. Rev. Lett. **109**, 107003 (2012).
[4]P. W. Anderson, J. Phys. Chem. Solids **11**, 26 (1959).
[5]D. Shahar and Z. Ovadyahu, Phys. Rev. B **46**, 10917 (1992).
[6]C. A. Marrache–Kikuchi, H. Aubin, A. Pourret, K. Behnia, J. Lesueur, L. Berge, and L. Dumoulin, Phys. Rev. B **78**, 144520 (2008).
[7]S. Okuma, T. Terashima, and N. Kokubo, Solid State Commun. **106**, 529–533 (1998).
[8]E. Bielejec and W. Wu, Phys. Rev. Lett. **88**, 206802 (2002).
[9]T. I. Baturina, D. R. Islamov, J. Bentner, C. Strunk, M. R. Baklanov, and A. Satta, JETP Lett.**79**, 337–341 (2004).
[10]N. Hadacek, M. Sanquer, and J.-C. Villegier, Phys. Rev. B **69**, 024505 (2004).
[11]T. I. Baturina, C. Strunk, M. R. Baklanov, and A. Satta, Phys. Rev. Lett. **98**, 127003 (2007).
[12]B. Sacepe, C. Chapelier, T. I. Baturina, V. M. Vinokur, M. R. Baklanov, and M. Sanquer, Phys. Rev. Lett. **101**, 157006 (2008).
[13]T. I. Baturina, J. Bentner, C. Strunk, M. Baklanov, and A. Satta, Phys. B: Condens. Matter **359–361**, 500–502 (2005).
[14]T. I. Baturina1, A. Yu. Mironov, V. M. Vinokur, M. R. Baklanov, and C. Strunk, Phys. Rev. Lett. **99**, 257003 (2007).
[15]V. M. Vinokur, T. I. Baturina, M. V. Fistul, A. Y. Mironov, M. R. Baklanov, and C. Strunk, Nature **452**, 613 (2008).
[16]W. Escoffier, C. Chapelier, N. Hadacek, and J.-C. Villegier, Phys. Rev. Lett. **93**, 217005 (2004).
[17]J. F. Creemer, D. Briand, H. W. Zandbergen, W. van der Vlist, C. R. de Boer, N. F. de Rooij, and P. M. Sarro, Sens. Actuators, A **148**, 416–421 (2008).
[18]N. D. Ashcroft and N. D. Mermin, *Solid State Physics* (Brooks & Cole, 1976).
[19]J. J. A. Baselmans, S. Yates, P. Diener, and P. de Visser, J. Low Temp. Phys. **167**, 360–366 (2012).
[20]J. Gao, J. Zmuidzinas, B. A. Mazin, P. K. Day, and H. G. Leduc, Nucl. Instrum. Methods **559**, 585–587 (2006).
[21]C. Walker, J. Matthew, C. Anderson, and N. Brown, Surf. Sci. **412**, 405–414 (1998).
[22]M. Tinkham, *Introduction to Superconductivity* (McGraw-Hill, New York, 1996).
[23]M. R. Vissers, J. Gao, D. S. Wisbey, D. A. Hite, C. C. Tsuei, A. D. Corcoles, M. Steffen, and D. P. Pappas, Appl. Phys. Lett. **97**, 232509 (2010).
[24]R. Barends, H. L. Hortensius, T. Zijlstra, J. J. A. Baselmans, S. J. C. Yates, J. R. Gao, and T. M. Klapwijk, Appl. Phys. Lett. **92**, 223502 (2008).
[25]S. Bose, P. Raychaudhuri, R. Banerjee, P. Vasa, and P. Ayyub, Phys. Rev. Lett. **95**, 147003 (2005).
[26]J. Halbritter, Phys. Rev. B **46**, 14861 (1992).
[27]J. Halbritter, Solid State Commun. **34**, 675–678 (1980).
[28]W. Splengler, R. Kaiser, A. N. Christensen, and G. Muller-Vogt, Phys. Rev. B **17**, 1095–1101 (1978).
[29]J. Halbritter, Z. Phys. **266**, 209–217 (1974).
[30]J. Gao, J. Zmuidzinas, A. Vayonakis, P. Day, B. Mazin, and H. Leduc, J. Low Temp. Phys. **151**, 557–563 (2008).
[31]D. E. Oates, A. C. Anderson, C. C. Chin, J. S. Derov, G. Dresselhaus, and M. S. Dresselhaus, Phys. Rev. B **43**, 437655 (1991).
[32]P. J. de Visser, J. J. A. Baselmans, P. Diener, S. J. C. Yates, A. Endo, and T. M. Klapwijk, Phys. Rev. Lett. **106**, 167004 (2011).
[33]B. Spivak, P. Oreto, and S. A. Kivelson, Phys. Rev. B **77**, 214523 (2008).